

Structure and Morphology of Biaxially Oriented Films of Polyethylenes

M. Kojima and J. H. Magill*

School of Engineering, University of Pittsburgh, Pittsburgh, Pennsylvania 15261

J. S. Lin

Oakridge National Laboratory, Oak Ridge, Tennessee 37831

S. N. Magonov

Digital Instruments, Santa Barbara, California 93103

Received September 27, 1996. Revised Manuscript Received December 11, 1996[®]

Biaxially oriented films of commercial polyethylenes were investigated using X-ray diffraction in directions transverse and perpendicular to the film plane. The surface morphology of the inner and outer faces of these films were studied in two directions by (a) transmission electron microscopy employing replication procedures, (b) by atomic force microscopy (tapping mode) down to nanometer resolution, (c) scanning electron microscopy of ion-etched metal coated surfaces, and (d) small-angle X-ray scattering measurements obtained from the bulk films. Discernible differences in morphological features were found for the inner and outer film faces that experienced different conditions during blow extrusion. The mean surface roughness of the films was measured and correlated with the haze parameters of these polyolefin materials. Trends in surface roughness with crystallinity (assessed from other measurements) are attributed to surface lamellar-like crystallization.

1. Introduction

The optical properties of polyolefin films have been investigated for approximately a half century.^{1,2} The source of haze formation (i.e., absence of clarity) has featured prominently in many of these studies, not only because of commercial interest associated with polymer processing but also for academic reasons.

Properties and film appearance determine marketability since quality production comprises a large percentage of polyolefin production. A clear understanding of the origin and mechanism of film haze formation should lead to its better control for this important sector of the polymer industry. Besides, biaxial film deformation leads to property improvements such as (1) improved mechanical properties and (2) reduced heat distortion even in materials that are noncrystallizable such as polystyrene, polycarbonate, and poly(methyl methacrylate). Of course, there are other applications where orientation is detrimental rather than beneficial particularly in lenses, optical storage disks, and other devices.

Several publications^{3–7} ascribe haze formation to surface roughness. It has also been reported that (i) crystallization, (ii) die flow instabilities, (iii) film line

disturbances, (iv) processing rates, and (v) material variables (induced or implicit) play a role too. In situ “on-line” investigations have been made of extrusion-blown film processing of diverse polymers where molecular weight, molecular weight distribution, or nucleants and processing variables have been studied.^{5–7} Haze formation in already processed films has also been attributed to surface roughness^{5–7} as a primary cause of haze. This conclusion was drawn from the observation that polymer films of relatively high crystallinities (the polyolefins) are opaque, whereas noncrystalline films are highly transparent. Now that modern microscopic techniques with image processing have facilitated surface imaging of materials^{8,9} to varying degrees of sophistication, we have attempted to merge information from novel^{8,9} and established^{5–7} methods to examine the surface morphology of three widely different polyethylenes. White et al.⁶ and others have made a nice presentation of surface transmittivity, T_s , against surface roughness, σ , for several polyethylene films. Bheda and Spruiell⁷ made quantitative studies of polypropylenes. The film transmission, T , has been related to the surface transmission factors T_{SO} (outer surface), T_{SI} (inner surface), and T_B (interior or bulk phase) by Clampitt et al.⁴

$$T = T_B T_{SO} T_{SI} = T_B T_S \quad (1)$$

Very recently¹⁰ the molecular orientation of polyethylenes were investigated using SAXS and WAXS X-ray

[®] Abstract published in *Advance ACS Abstracts*, May 1, 1997.

(1) Norddentsche Seekabelwerke, British Patent 431,619, 1935.

(2) Park, W. R. R. *Encycl. Polym. Sci. Eng.* **1965**, 2, 339.

(3) Huck, H. D.; Clegg, P. L. *Trans. SPE* **1960**, 1, 121.

(4) Clampitt, B. H.; German, D. E.; Anspon, H. E. *Anal. Chem.* **1969**, 41, 1306.

(5) Stehling, F. C.; Speed, C. S.; Westerman, L. *Macromolecules* **1981**, 14, 698.

(6) White, J. L.; Matsukura, Y.; Kang, H. J.; Yamane, H. *Int. Polym. Processing* **1987**, 1, 83.

(7) Bheda, J. H.; Spruiell, J. E. *Polym. Eng. Sci.* **1986**, 26, 736.

(8) Quate, C. F. *Surf. Sci.* **1994**, 299/230, 980.

(9) Magonov, S. N. *Polym. Prepr.* **1996**, 37, 597.

(10) Pazur, R. J.; Prod'homme, R. E. *Macromolecules* **1996**, 29, 119.

(11) Stein, R. S.; Norris, F. H. *J. Polym. Sci.* **1958**, 27, 87.

Table 1

no.	specimen	ρ	total haze (%)	internal haze (%)	blow-up ratios
I	high-density polyethylene, HDPE	0.952	62.6	2.1	~4:1
II	linear low-density polyethylene,	0.917	31.2	4.3	2:1
II	LLDPE	0.926	10.2	1.8	2:1
I	low-density polyethylene (with vinyl acetate, 5%), LDPE				

pole figures for a range of film, spanning low to high blow-up conditions. From a practical viewpoint they concluded that their approach may be used to verify the quality and consistency of blown films in production scenarios.

2. Experimental Section

Materials. Three finished samples of polyethylenes with haze and density results were kindly provided by EXXON Chemical Co. with the information on haze and typical blow-up ratios. These are designated in Table 1.

3. Techniques

All microscope measurements were made at several magnifications in order to facilitate image interpretations.

3.1. Scanning Electron Microscopy. A JEOL JSM-5300, 20 kV SEM was used to examine the surface texture of these films after they were ion-bombarded in air and subsequently sputtered with Au/Pd metal in a vacuum. The inside and outside of each specimen were investigated for distinctive features that could be attributed to their formation. It is generally recognized during processing that in the inside of the tubular film the air is comparatively static, whereas the outer film surface is subjected to faster cooling and greater stress. An attempt was made to examine the affect of the biaxial constraints that facilitate surface and bulk crystallization in biaxially oriented films. Fresh sample surfaces were subjected to ion bombardment in air at a chamber pressure of 2×10^{-1} Torr, employing a JEOL JFC-1100 sputtering instrument where the current was maintained at 5 mA (ac) during the 40 min sputtering period used. Past experience¹² has taught us that this procedure delineates clusters of lamellae separated by empty spaces that are left after etching away the less ordered and amorphous polymer revealed as dark "voids" linked by a lighter network of crystallites. In Figures 1a–f, respectively, the inside and outside features of the three films are highlighted. In these examples, differences in texture are noted between the outside and inside surfaces. Presumably the original surface layer has been sputtered away by the ion bombardment. Differences still exist among the three types of films. Note the variations in the directions of the clusters or rows of transcrystallites that have their molecular chain, *c*, axis aligned essentially perpendicular to these stacked layered regions, established here according to electron diffraction evidence here and also reported elsewhere.¹² In addition, distinct topographical features are distinguishable from one type of polymer to another. This appears to us to be the real function of the etching process. The HDPE film displays

features that are consistent with its higher crystallinity and haze compared with the LDPE (5% VA) sample. The density of LDPE is marginally higher than that of LLDPE. The "cluster" dimensions in these micrographs are best defined for HDPE film and measure 200–305 nm (inside) and about 250–350 nm (outside). For LLDPE film, clusters are in the range 150–200 nm (inside) to about 200–250 nm on the outside of this film surface. For the lowest crystallinity and most transparent LDPE (5% VA) film there is insufficient relief in the image to comment more meaningfully on these differences, but an estimate of the etched inner surface that has particles (presumably crystallites) range from about 200 nm upward. Note that all of these dimensions are about an order of magnitude larger than the values determined by TEM, SAXS, and AFM techniques, respectively. Perhaps it is worth noting that there are also periodic features present on an otherwise "smooth" outside surface as seen in Figure 2e. Barely discernible in Figure 1a,e,f is a finer texture (arrowed), running for small distances along the length of the crystalline clusters, but they cannot be reconciled with a specific morphology at present.

3.2. Transmission Electron Microscopy (TEM). Carefully conducted investigation of the three films were made using carbon one-step replicas after Pd/Au shadowing, followed by peeling the carbon film off the specimen surface. The granularity of the Pd/Au sputtering was checked at high magnification to ensure it did not interfere with the measurements obtained here. Typical replicas for the inside and outside faces of HDPE film are shown in Figure 2a,b. Row nucleated lamellae or crystallites are well aligned in specific directions that must mimic the stressed crystallized melt with the *c* axis aligned in this direction. The rows of nuclei follow different directions commensurate with the biaxial stresses during processing of the film. Typical micrographs obtained from inside and outside the crystallized film illustrate their surface texture. The mean crystallite spacing on the inside ranges between 20 and 30 nm and on the outside more than one direction of row nucleation is apparent, the spacing ranges between about 25–40 nm and even larger, since crystallites are tilted in many areas so that estimations are difficult to make. In some places, the lamellae appear to be twisting much as they do in spherulitic growth, but this morphology is out of the question since spherulites are absent in these films.

In LLDPE, the thin lamellae are recognizable but are located (nucleate) in clusters where they intermingle and are oriented in different directions. There is multiple nucleation as is often reported in trans spherulitic nucleation/growth, but there is a distribution of asperities to be found on the inside as well as outside film surfaces, although on the inside surface, they are more concentrated, as in Figure 2e. A rough estimate of the periodicity associated with crystallites is 35–50 nm. On the outside surface (Figure 2d) the asperities

(12) Kojima, M.; Satake, H.; Shankernarayanan, M. J.; Magill, J. H. In *Morphology of Polymers*; Sedlacek, B., Ed.; Walter de Gruyter and Co.: Berlin, 1989; p 279.

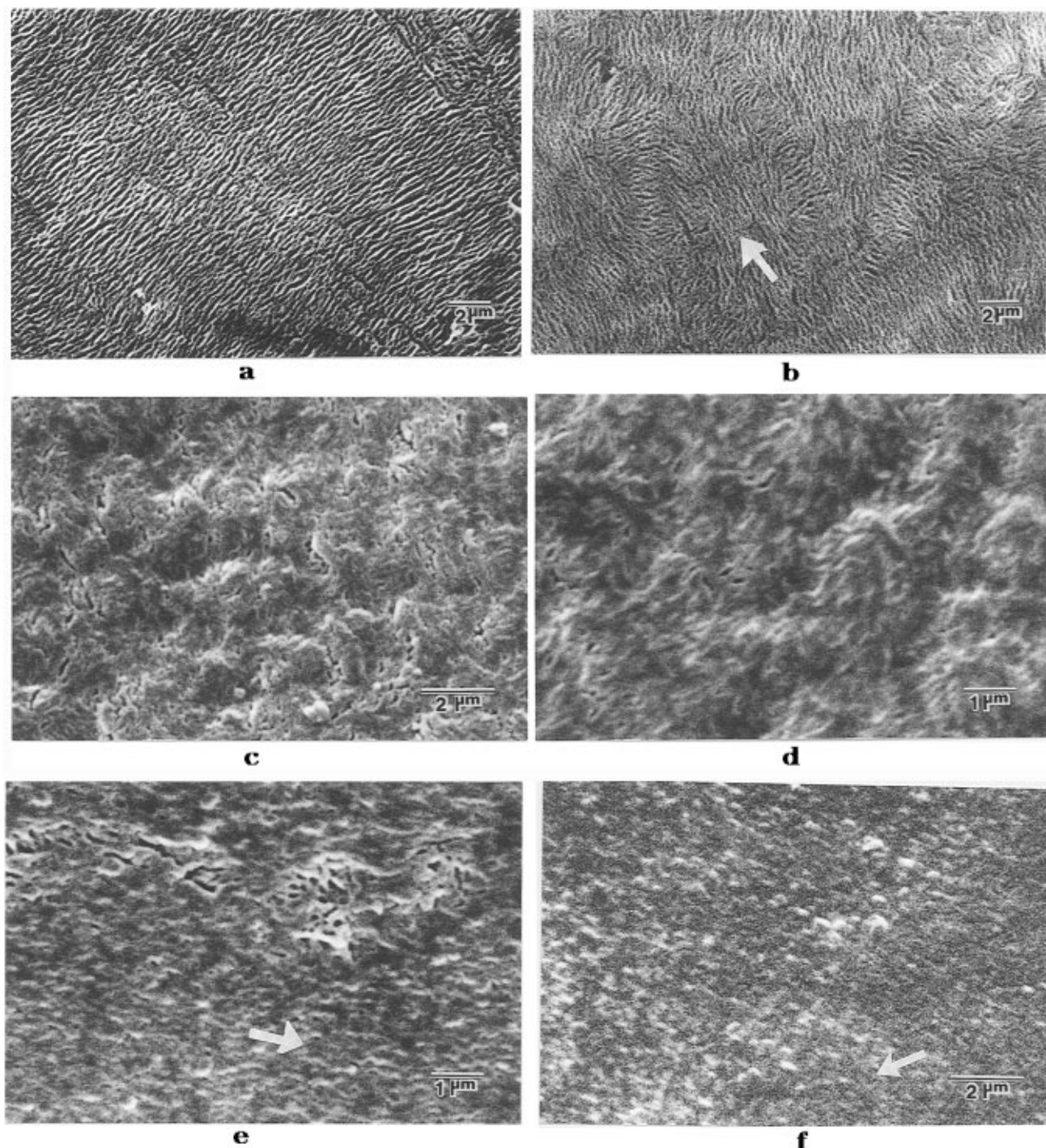


Figure 1. Biaxially oriented films surface etched in air atmosphere for 40 min at 5 mA (AC) using a JEOL JFC-1100 sputtering instrument. Specimens were examined by means of a JEOL JSM-5300, 20 kV scanning electron microscope: (a) inside HDPE film; (b) outside HDPE film; (c) inside LLDPE film; (d) outside LLDPE film; (e) inside LDPE (5% VA) film; (f) outside LDPE (5% VA) film.

appear larger and one might speculate that they are also shallower. Crystallites tilt and change direction erratically, bearing some evidence of nucleation centers that are reminiscent of spherulitic nucleation! A rough estimate of their size stands at 40–60 nm, again with some lamellar tilting involved. This complicates the measurements. The LDPE (5% VA) films inside and outside (Figure 2e) were almost featureless from a lamellae or crystallite size viewpoint, so that meaningful estimates of size were very difficult to make.

Other supporting observations were made on these three films. Using a Leitz polarizing microscope and crossed-polars (up to 600 \times magnifications) revealed that

spherulites were absent. However, the films did exhibit preferred orientation which was most pronounced in the HDPE specimen. This observation was commensurate with the “blow-up” condition of their formation. Correspondingly, supportive results were obtained for the light scattering H_v and V_v observations with a laser assembly (not shown).

It has been reported¹⁰ that the scattering power of a polymer strongly depends upon orientation, the more highly oriented films exhibiting less scattering than unoriented material, presumably as a consequence of the decrease in fluctuations in local index of refraction in the sample. According to eq 1, the bulk transmission,

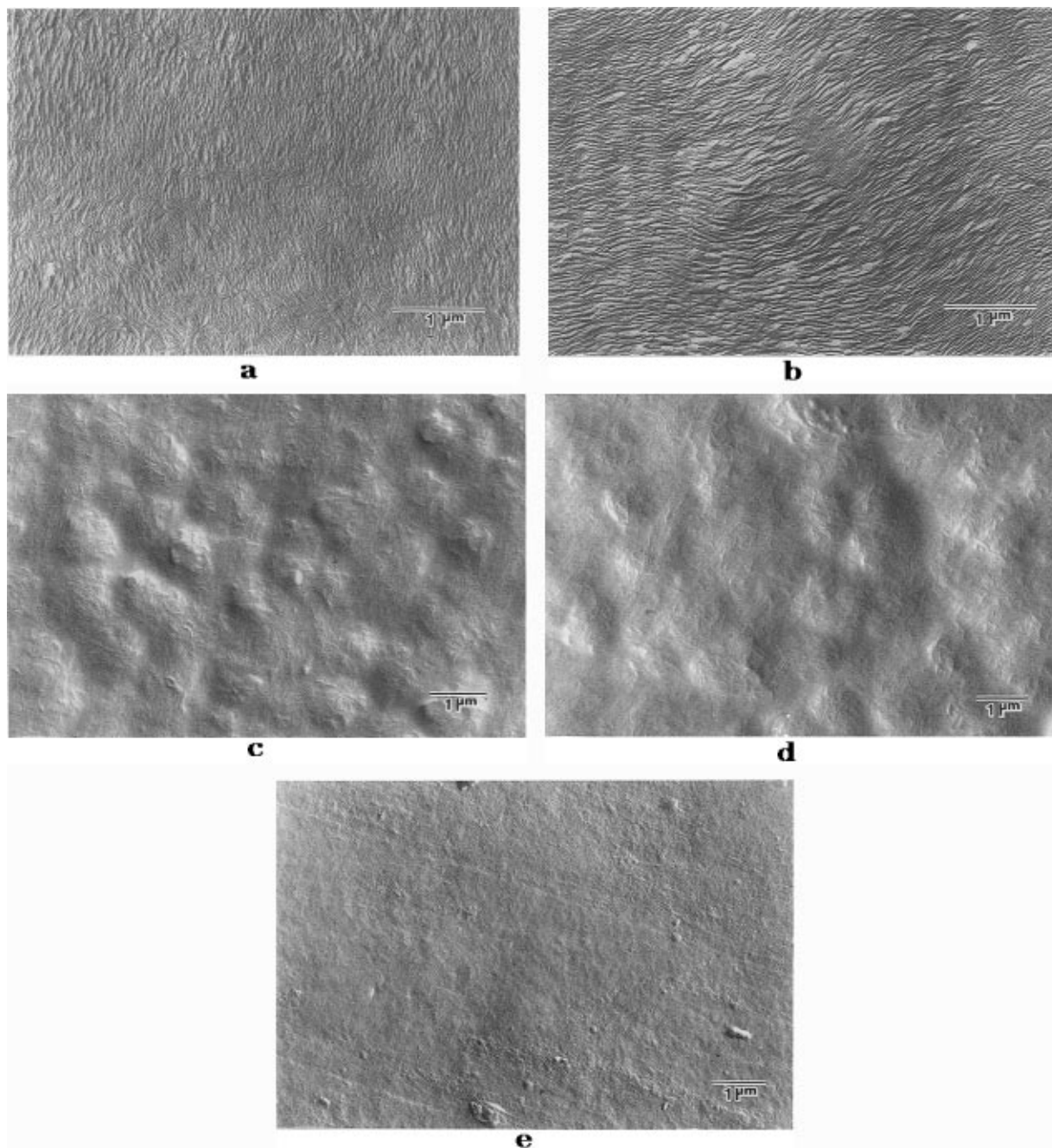


Figure 2. TEM Philips CM30 200 kV micrographs of carbon one-step replicas: Pd/Au shadowed for biaxially oriented: (a) inside HDPE film; (b) outside HDPE film; (c) inside LLDPE film; (d) outside LLDPE film; (e) outside LDPE (5% VA) film.

T_b , is less than the total transmission, T , which contributes most to the scattering. Elsewhere, it has been noted⁷ that spherulite size alone does not control the intensity of scattered light or T_b , even though correlations do exist between spherulite radius and internal size.

3.3. Small-Angle X-ray Scattering. The 10 m SAXS Facility¹³ at the Oak Ridge National Laboratory was used to carry out experiments on the three polymer films. Scattering experiments using Cu K α radiation of 40 kV and 40 mA were conducted at sample-to-detector distances (SDD) of 1.119 and 5.119 m, respectively. The most satisfactory results were obtained at the longer SDD. Absolute intensity measurements were

carried out on multilayers of films of the three specimens carefully cut and mounted in accordance with recognized procedures.

Because of the biaxial orientation of these films, diffraction measurements were made perpendicular to the film plane and in the other two mutually perpendicular directions. It was not possible to examine the inside and outside surfaces of the films conveniently by SAXS. Surface and bulk features were not distinguished so that only an average dimension resulted from the peak position of the scattering curve for each polymer sample. The location of the peak maximum in the intensity plots of $Q^2 I(Q)$ vs Q and also $I(Q)$ vs Q plots were made for each film. Small differences are observed within, as well as significant ones between samples, as displayed in Figure 3. The long period (L) is comprised of the crystalline, l_c , and amorphous

(13) Wignall, G. D.; Lin, J. S.; Spooner, S. J. *Appl. Cryst.* **1990**, *23*, 241.

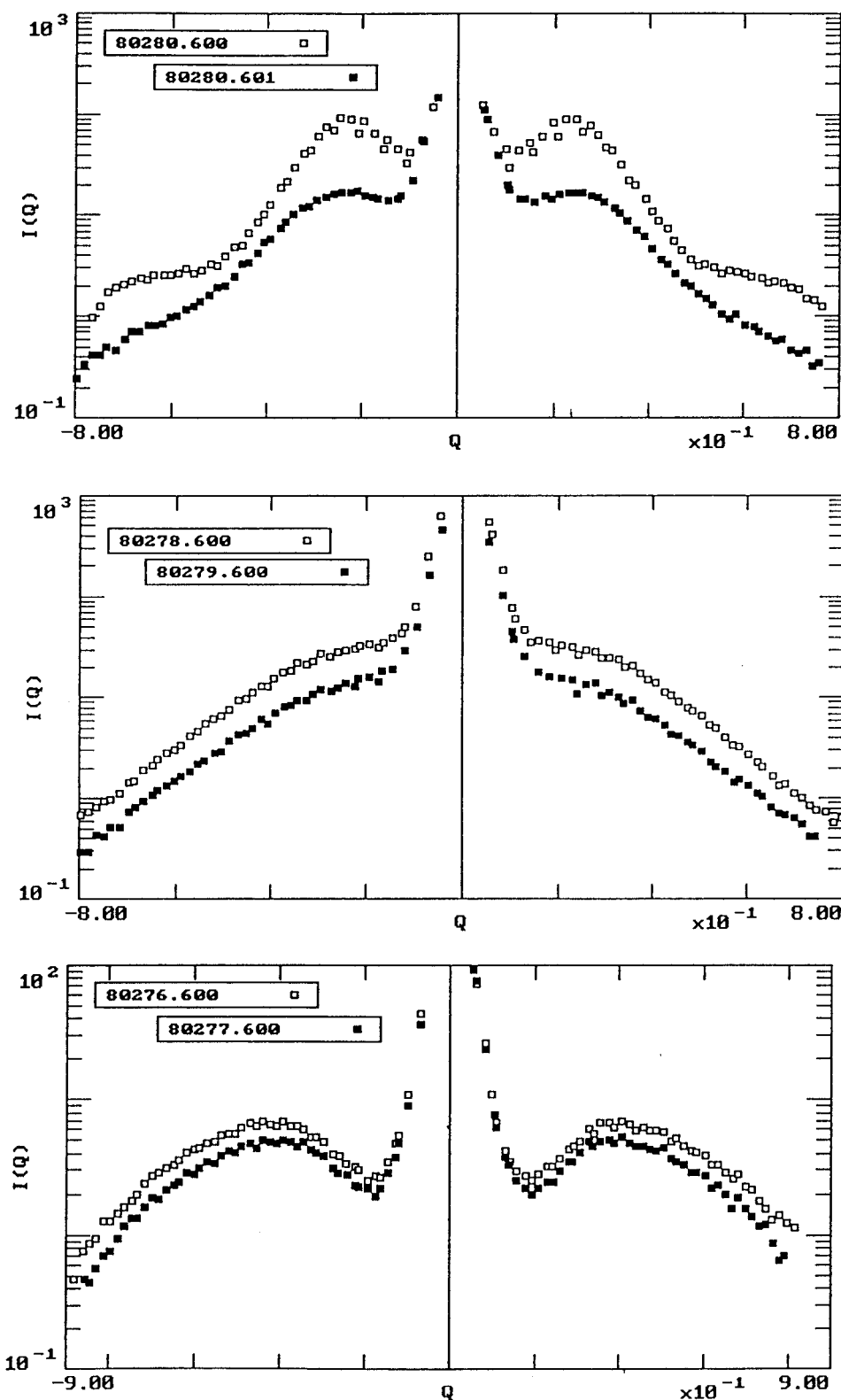


Figure 3. Small-angle X-ray diffraction plots of biaxially oriented film sample to detector distance 5.119m; radiation Cu K α at 40 kV, 40 mA: (a) (i) perpendicular to HDPE film (\square), (ii) parallel to HDPE film (\blacksquare); (b) (i) perpendicular to LLDPE film, (ii) parallel to LLDPE film; (c) (i) perpendicular to LDPE (5% VA) film, (ii) parallel to LDPE (5% VA) film.

contributions, I_a , provided in Table 2. Of course, this is a simplistic view of the morphology because there must also be oriented amorphous material in these specimens, and it awaits other investigations.

The intensity of the scattering peak (Figure 3a) perpendicular to the HDPE is considerably sharper and more intense (almost an order of magnitude) than the scattering recorded parallel to the same film depicting

Table 2. Comparison of Long-Period Data for Each Polyethylene

sample	long period (nm)
HDPE	29
LLDPE	26
LDPE (5% VA)	20

a change in internal morphology in these two directions. Presumably, there is a directional difference in electron

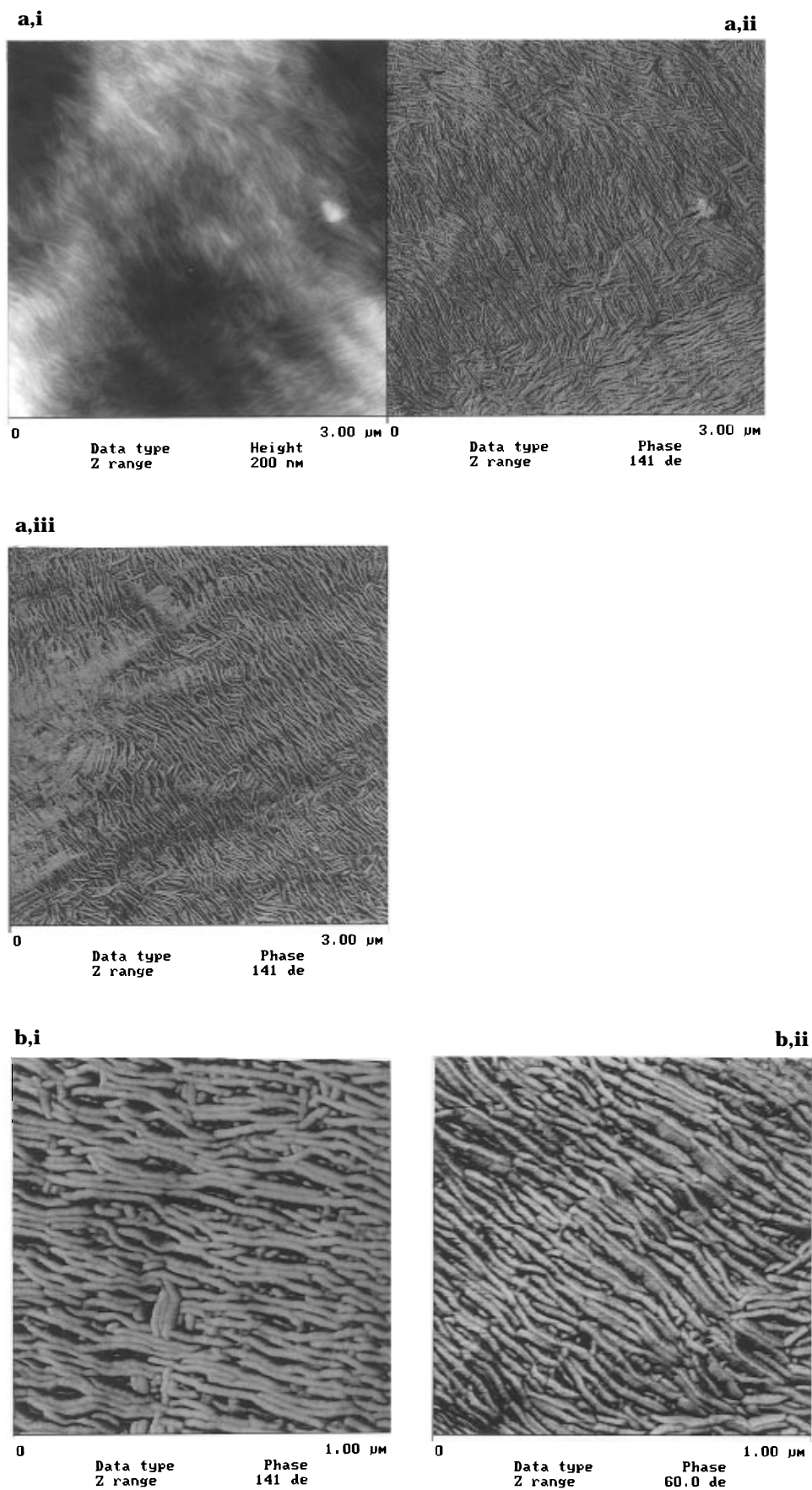


Figure 4.

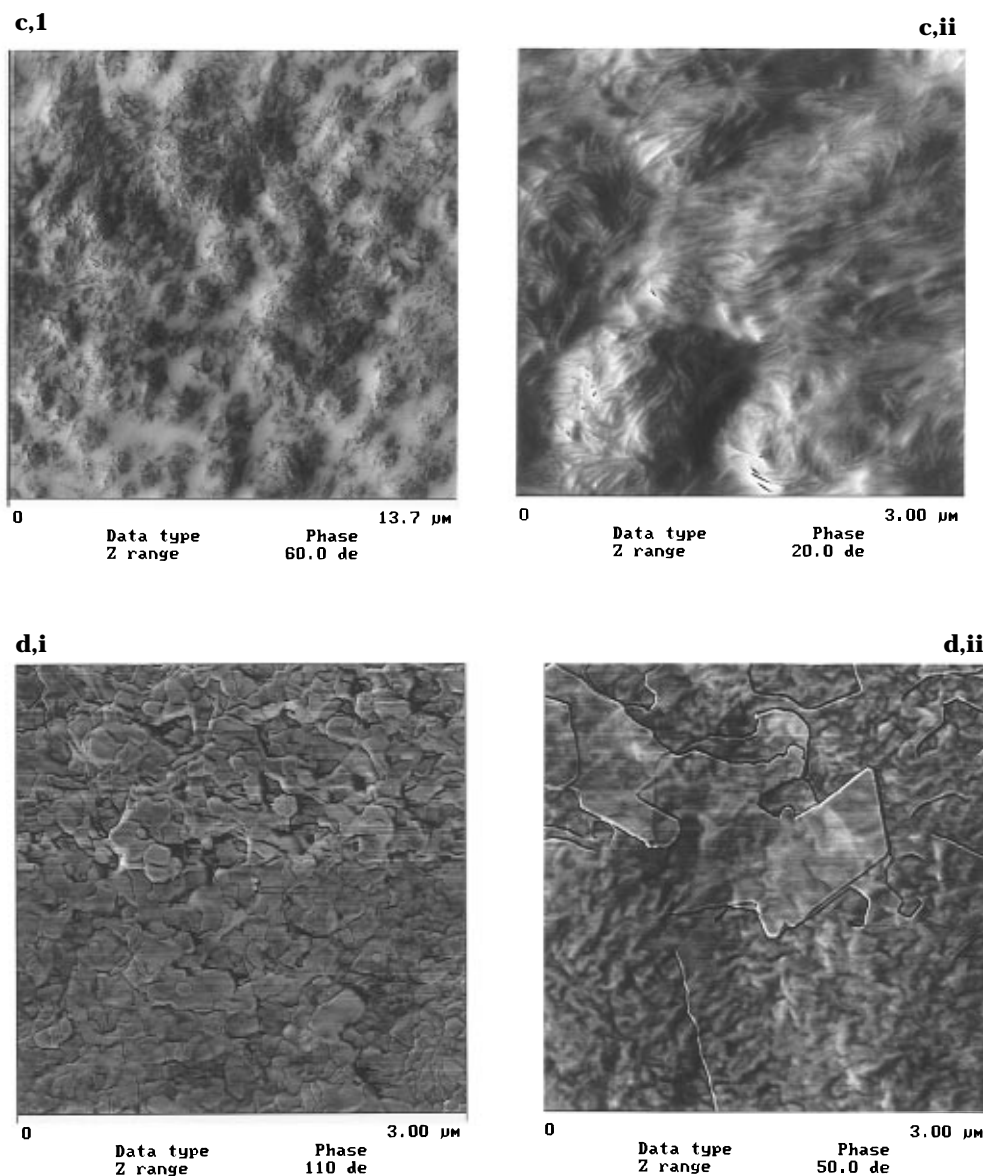


Figure 4. Atomic force microscopy micrographs of polyethylene film surfaces: (a) (i) height and (ii) phase images for HDPE inside surface (iii) phase image for outside HDPE surface; (b) phase images for (i) inside and (ii) outside HDPE surfaces; (c) phase image of LLDPE inside surface at (i) low and (ii) higher magnification; (d) phase images of LDPE (5% VA) (i) inside and (ii) outside surfaces.

Table 3. Topological^a and Bulk Features of Polyethylene-Blown Films

sample	haze	long period L (nm) ^c	TEM (replica)		SEM (ion-etched) ^b		AFM	
			inside	outside	inside	outside	inside	outside
HDPE	62.6	29 (22)	20–30	25–40	200–250	250–350	18–22	23–28
LLDPE	31.2	26 (18)	35–50	40–60	150–200	200+	20–25	25–35
LD (5% VA)	10.2	20 (12)			~200			10–40 clusters

^a All microscopic dimensions are given in nanometers. Haze is expressed as a percentage. Other dimensions (surface and bulk) are expressed in nanometers and rounded to the nearest nanometers. A blank in the table signifies that no meaningful result was possible.

^b In this case, ion bombardment of the surface removes the outer film surface so that the features revealed hardly correspond to the morphology of the true film surface initially formed. ^c Values for L are determined from $Q^2I(Q)$ vs Q plots.

density due to anisotropic stretching. The scattering intensity curves (Figure 3b) from the less-crystalline LLDPE film is of lower intensity but similar in shape in the perpendicular and parallel directions. A clearer pattern of the peak position can be obtained from $Q^2I(Q)$ vs Q plots, although this induces the peak to move to smaller L values shown in Table 3.

For the polyethylene copolymer with 5% VA, again the scattering curves are similarly disposed, the intensity perpendicular to the film is higher than it is in the

parallel direction to the film, as Figure 3(c) demonstrates. Note that a discrete scattering peak is associated with the bulk crystallization in all three polyethylenes. It is somewhat surprising to us that the copolymer (with 5% VA) exhibits a relatively sharp SAXS peak, but it is essentially featureless in all surface measurements.

3.4. Atomic Force Microscopy. AFM measurements were performed with a Nanoscope IIIa (Digital Instruments, Inc., Santa Barbara, CA) in the tapping

mode with simultaneous recording of the height and phase images. Imaging was conducted by using Si probes with resonant frequencies in the 150–180 kHz range. Measurements were made on the inside and outside surfaces of each polyethylene film at a series of magnifications in order to assist in the morphological interpretations. The tapping mode was employed in order to minimize surface damage. Height images were recorded, and the contrast was directly related to surface roughness. Phase images were also obtained where morphological details were better highlighted due to the improved contrast that obtains here. With broadening AFM applications, it becomes evident that when experiments are conducted at different tip force, the height and phase images exhibit contrast related to local sample stiffness and adhesion.⁹

Each of the three samples showed distinct but recognizable morphological features. In the case of the HDPE polymer film, both surfaces were comprised of lamellar arrays, and the width of individual lamellae ranged from 18 to 22 nm approximately on the inside HDPE surface. On the outside surface of the film, it is a little higher, about 23–28 nm, from Figure 4a. The orientation overall is more prominent generally on the outside surface. At low magnification, crystallites (not shown) are sometimes aligned like shishkebabs with their molecular chain direction lying in the “blow-up” direction corresponding to the stressed melt crystallization regions within the specimens. In the AFM height and phase images (Figure 4), these clusters assume diverse directions. Besides being aligned in “runs” of lamellae several micrometers in length in some areas, there are “runs” of crystallites essentially perpendicular to some others with many mixed directions between these extremes. The length of the crystallites (perpendicular to the *c* axis direction often reach 1 μm with the majority a fraction (about 0.2 μm) of this length. Outside of the film the runs of crystallites seem to be aligned in representative samples. Anyhow, at the higher magnifications, Figure 4a,i,ii illustrates that the phase images are favored over the surface height so far as details are concerned. Some crystallites (Figure 4b,ii) appear to have serrated edges that run along their lengths that span from 0.05 to 0.5 μm . Besides, they appear to contain “fine structure internally” within their 20 nm thickness, but a satisfactory explanation cannot be advanced for these features at this time. The crystallites appear featherlike, for lack of a better description. On average, the crystallites (inside face) have dimensions ranging from 18 to 22 nm, whereas the one outside has dimensions from 23 to 28 nm for HDPE. The inside lamellae are rounded and have fewer fine features.

In the LLDPE film, there is clear evidence of crystallites that are usually clustered and curved in several directions at lower magnification in the inside of the film (Figure 4c,i). At higher magnification (Figure 4c,ii), these crystallites are considered to be splayed within and among clusters. The outside micrograph (Figure 4d,ii) of the film in the phase mode shows the surface to be comprised of well-defined lamellae that are better regulated, with respect to each other, but are still oriented in several directions. A crude estimate of their thickness is about 20–25 and 25–35 nm for the inside and outside surfaces of the film, respectively. There are

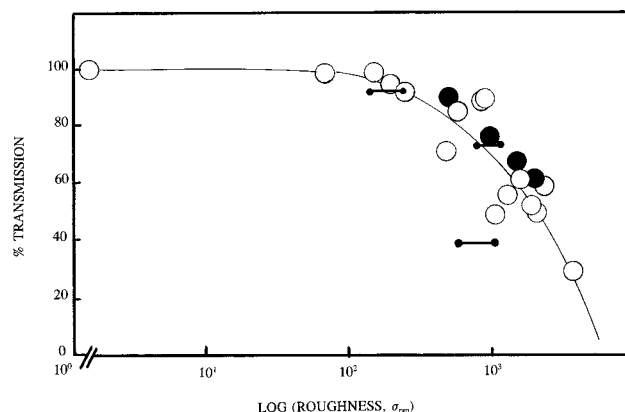


Figure 5. Plots of percent transmission vs log (surface roughness) for several polymer films for this investigation (dumbbell notation). Data from ref 6 on polyethylenes (open circles) and ref 7 deals with polypropylenes (dark circles) are included for comparison.

no distinct directionally ordered transcrystalline features that are comparable with those noted for the HDPE sample.

For the LDPE (5% VA) films, the height image is much less detailed and indistinct than the phase image although a sense of height is discernible. Oddly, the phase image (Figure 4d,ii) exhibits faceted features (presumably an impurity) that has “bloomed” and crystallized on the outside of the film. Besides this “oddity” the phase image depicts variously shaped clusters ranging in size from ~10 to 40 nm, and they can be anticipated as exhibiting a crystalline nature. Even so, the surface features are not as distinct on the inside of the film (Figure 4d,i), which tends to be mostly featureless. The surface topography of this sample was the most difficult to assess for this series of polyethylenes.

For other copolymers such as LLDPE and styrene–butadiene–styrene triblock copolymer (Magonov, unpublished), there is some evidence for a thin topmost surface layer of amorphous PE and of amorphous butadiene-rich materials, respectively. These layers are seen only in the low force images, but with the increase tip force the underlying structures (PE lamellae and microphase-separated patterns) appeared in the height and phase images. This observation demonstrates a possibility to examine near-surface structure in polymer samples with AFM.

3.5. Surface Roughness. These measurements were obtained from AFM scans carried out over various inner and outer surfaces of the films. Typical surface profiles were made as linear scans across the crystallites as well as from several boxed/mapped areas of each of the film surfaces. Root-mean-square statistics and mean roughness values were estimated for each sample surface by using “off-line” procedures documented in the Nanoscope Command Reference Manual (no. 12-67) to acquire the representative values (dumbbell data points) that are plotted in Figure 5.

4. Discussion

The long periods of these polyethylenes were readily assessed from SAXS measurement where the averaged long period (amorphous and crystalline dimension) of the films is heavily weighted in favor of the bulk

morphology. The L values in Table 2 are in the order

$$\text{HDPE} > \text{LLDPE} > \text{LD (5\% VA)}$$

and each comprise an average crystallite dimension contributed by the amorphous/crystalline periodicity of the bulk material. These L values provide a yardstick against which other values in this work may be gauged.

Replicated TEM micrographs from inside and outside of each of the film surfaces provide crystallite dimensions that compare favorably with the AFM images, particularly those obtained by means of the phase imaging technique. Similar, but less distinct features are found in the surface height images but the correspondence is still obvious, except for the copolymer. Note that the AFM topography and TEM replicas for LLDPE portray similar overall surface features and nucleation events of comparable magnitude and distribution. The SEM micrographs of the ion-etched polyethylenes without exception, exhibit dimensions that are an order of magnitude larger than the lamellar sizes determined by the other techniques. It would appear that the surface lamellae cluster or collapse together forming larger crystalline aggregates without altering the " c " axis orientation after the coexisting amorphous material is removed. Table 3 summarizes some of the pertinent data obtained for comparison of the three polyethylenes. In line with current conceptions, it seems that haze and surface roughness are not at variance. Visual inspection of corresponding TEM replicated surfaces and AFM scanned materials are comparable as the tabulated measurements (Table 3) show. Ion-etched materials could benefit from closer scrutiny as to their true morphology. They do not provide a clear concept of lamellar thickness, but it is noteworthy that the c axis orientation is maintained, as assessed by electron diffraction from detached thin layers of the etched surface.¹²

Figure 5 is a plot of the percent transmission vs surface roughness obtained in this investigation. The

plot is presented alongside published data obtained for other polyethylenes⁶ and polypropylenes.⁷ In all examples, there is a downward trend in transmission with enhanced roughness (arising from crystallites that are located in the respective surfaces). A new study¹⁴ made on poly(ethyleneterephthalate) biaxially oriented film (containing 1 μm particle) has demonstrated that these moieties concentrate in the surface and induce surface roughness. In line with this notion and despite that there may be other contributory factors, it is concluded that surface roughness dominates haze production and that it strongly correlates with the crystalline features of the film surfaces.

Conclusions

The surface analysis techniques employed in this investigation leads one to conclude that surface crystallites are responsible for polymer film haze.

The surface investigated by AFM and direct TEM replication and the inner bulk morphological features (from SAXS measurements) are of comparable dimensions. However, the dimensions obtained from ion-etched surfaces grossly overestimates the basic crystallite sizes obtained by the other techniques, even though the c axis orientation direction in the etched and unetched samples are the same.

Acknowledgment. This project was supported in part by the Division of Materials Sciences, U.S. Department of Energy, under Contract No. DE-AC-05-96OR22464 with Lockheed Martin Energy Research Corp. Co. The authors wish to thank Dr. Gerry Wissler and Donna Terry of the Exxon Chemical Co. for providing the characterized samples used in this work.

CM960505H

(14) Khan, M. B.; Keenan, C. *Polym. Eng. Sci.* **1996**, 36, 1290.